JAST, Vol. 2, No. 2, pp 1–9

JAST
Journal of Aerospace Science and Technology

Investigation of Three-Dimensional Turbulent Cavity Flow Using Large Eddy Simulation Approach

Mohammad Taeibi-Rahni[1], Mahdi Ramezanizadeh[2]

Large eddy simulation (LES) of an incompressible flow in a three-dimensional cavity at different Reynolds numbers including 3,200 and 10,000 are performed using Smagorinsky subgrid scale (SGS) model. Our computational methodologies include finite volume method using unsteady SIMPLE algorithm, employing a non-uniform staggered grid. All terms in the Navier-Stokes equation were discretized using Power-Law scheme. Here, the mean and root-mean-square (rms) velocities are shown in horizontal, vertical and spanwise coordinates passed through the center of the cavity and are compared with the experimental results of Prasad and Koseff (1989). Also, the ratios of turbulent viscosities to kinematic viscosity are calculated and the position of the maximum ratio is determined. Although, the Smagorinsky model does not work well near the walls, this comparison shows reasonably good agreements and it is able to resolve the dynamically significant scales of the flow within the approximations.

INTRODUCTION

Turbulence is a phenomenon that occurs frequently in nature; it has, therefore, been the subject of study for over one hundred years [1]. Most engineering and environmental flows are turbulent, and occur in geometrically complex domains. In direct numerical simulation (DNS) of the Navier-Stokes (NS) equation, the numerical resolution is sufficiently fine in order to resolve all scales of motion carrying significant energy. It is well known that such resolution requirements make DNS prohibitively expensive for most applications, and it is restricted to low and moderate Reynolds number flows. On the other hand, the Reynolds averaged Navier-Stokes (RANS) approach, which is much cheaper computationally, uses non-universal closure models. An intermediate approach is large eddy simulation (LES), where one only seeks to resolve those eddies that are large enough to contain information about the geometry and the dynamics of a specific problem under consideration. LES regards all flow structures on smaller scales 'Universal', following the point view of Kolmogorov [2].

The application of LES to turbulent flows consists of three separate steps. First, a filtering operation is performed on the Navier-Stokes equations to remove small spatial scales. The resulting equations describe the space-time evolution of the 'large eddies' including the subgrid scale (SGS) stress tensor that describes the effect of the unresolved small scales. In principle, the SGS stress tensor depends on the precise definition of the filtering operation and on the parameters characterizing it. The second step is the replacement of the SGS stress (which is unknown, since it depends on the unresolved scales) by a 'model'. The 'model' may be any expression, which can be calculated from the resolved scales and may or may not contain some adjustable parameters. The final step is the numerical simulation of the resulting 'closed' equations for the large scale fields on a grid small enough to resolve the smallest of the large eddies, but still much larger than the fine scale structures at the Kolmogorov scale level [3]. Here, we focus our attention on the third step, i.e., is using the LES method with the Smagorinsky

1. *Associate Professor, Department of Aerospace Engineering, Sharif University of Technology, Tehran, I.R Iran, E-mail: Taeibi-Rahni@Sharif.edu.*
2. *PhD Candidate, Department of Mechanical Engineering, Sharif University of Technology, Tehran, I.R. Iran, E-mail: Ramezanizadeh@mehr.sharif.edu.*

model to solve a three-dimensional time-dependent cavity flow.

GOVERNING EQUATIONS

The dimensionless Navier-Stokes equations for incompressible, three-dimensional, and, time-dependent flow in index notations are as follows:

$$\partial_i u_i = 0$$

$$\partial_t u_i + \partial_k(u_i u_k) = -\partial_i p + \frac{1}{\mathrm{Re}}\partial_{kk} u_i \tag{1}$$

The governing LES equations are obtained by filtering the above equations. Filtration is a process by which all scales smaller than a selected size (e.g., grid size) are eliminated from the total flow. It defines the resolvable part of the flow, and is accomplished by using a general filter function in space to limit the range of scales in the flow field. In one dimension, we have:

$$\bar{f}(x) = \frac{1}{\Delta x}\int f(x')G(x,x')dx'$$

$$\bar{f}(x) = f(x) - f^{sgs}(x) \tag{2}$$

where, $f^{sgs}(x)$ is the SGS component of the variable $f(x)$. Applying the above filter operation to the Navier-Stokes equations, we derive the LES equations as follows:

$$\partial_i \bar{u}_i = 0$$

$$\partial_t \bar{u}_i + \partial_k(\bar{u}_i \bar{u}_k) = -\partial_i \bar{p} + \frac{1}{Re}\partial_{kk}\bar{u}_i - \partial_j \tau_{ij} \tag{3}$$

The effects of the small scales are present through the SGS stress tensor:

$$\tau_{ij} = (\overline{u_i u_j} - \bar{u}_i \bar{u}_j) \tag{4}$$

which must be modeled [2].

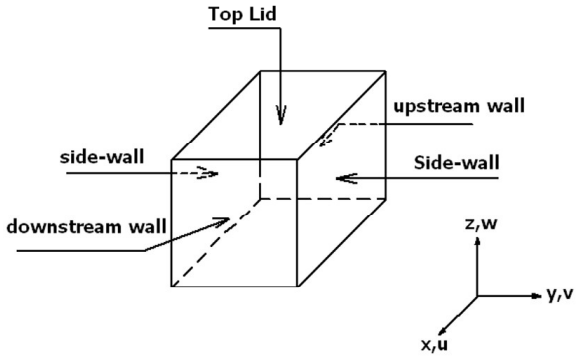

Figure 1. Geometry and boundary conditions of the Lid-driven cavity flow.

Subgrid Scale Model

The key to the success of LES is to accurately represent the resolved SGS stresses. There are a number of SGS models varying in complexity from eddy-viscosity to one-equation models. The most widely used model is Smagorinsky, which was suggested in 1963. This model is based on Boussinesq's approximation, in which the anisotropic part of the SGS stress tensor is related to the strain rate tensor of the resolved fields through an eddy-viscosity [4], i.e.,

$$\tau_{ij} - \frac{\delta_{ij}}{3}\tau_{kk} = -2\nu_t \bar{S}_{ij} \tag{5}$$

where, ν_t is the eddy-viscosity, which is computed from the resolved strain rate tensor magnitude and a characteristic length scale as:

$$\nu_t = l\left|\bar{S}\right| = C_s \bar{\Delta}^2 \left|\bar{S}\right| \tag{6}$$

where, l is a characteristic length scale and is assumed to be proportional to the filter width ($\bar{\Delta}$ via a Smagorinsky coefficient, C_s . In this research, C_s was considered to be 0.17, which was suggested by Lilly [5]. $\left|\bar{S}\right| = (2\bar{S}_{ij}\bar{S}_{ij})^{\frac{1}{2}}$ is the magnitude of the resolved strain rate tensor and,

$$\bar{S}_{ij} = \frac{1}{2}\left(\frac{\partial \bar{u}_i}{\partial x_j} + \frac{\partial \bar{u}_j}{\partial x_i}\right) \tag{7}$$

Table 1. Parameters of the cases run in the present study.

Case	$\mathrm{Re} = \frac{U_B L_x}{\nu}$	Grid Points(x, y, z)	$\Delta x_i / L_i$	L_i (x, y, z)
1	3200	$35 \times 35 \times 35$	2×10^{-2}	$1.0 \times 1.0 \times 1.0$
2	10000	$65 \times 33 \times 65$	1.5×10^{-2}	$1.0 \times 0.5 \times 1.0$

Table 2. The applied grid arrangements for the grid resolution study of case 2.

Grid	Grid Pointsx,y,z	Minimum Grid Spacing	MaximumGrid Spacing
1	$33 \times 17 \times 33$	0.0099	0.05217
2	$49 \times 25 \times 49$	0.00641	0.03484
3	$65 \times 33 \times 65$	0.00474	0.02614
4	$81 \times 41 \times 81$	0.003761	0.02092

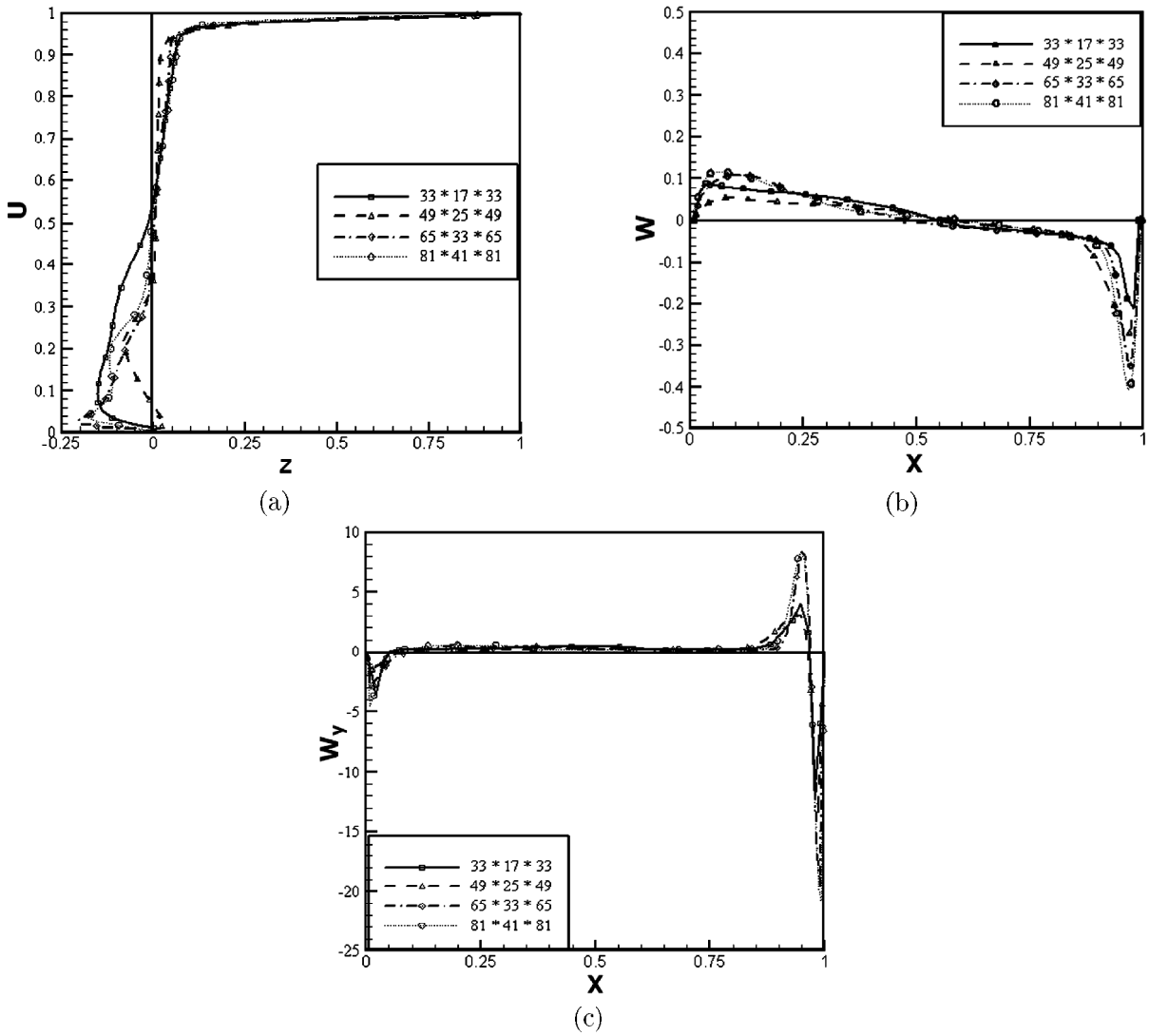

Figure 2. Grid resolution study profiles at different centerlines for case 2: (a) streamwise velocity profile at x=0.5; y=0.25 line, (b) vertical velocity profile at y=0.25; z=0.5 line, and (c) lateral vorticity profile at y=0.25; z=0.5 line.

Note, in the classical Smagorinsky model with a constant C_s , the concept of a filter is required and one does not need to know how exactly it is defined because one does not need to use the filtering operation explicitly in solving the basic equations [2]. The SGS stresses can be decomposed into three parts Leonard, Cross, and, Reynolds shown below:

$$\tau_{ij} = \overline{u_i u_j} - \bar{u}_i \bar{u}_j = L_{ij} + C_{ij} + R_{ij} \tag{8}$$

where,

$$L_{ij} = \overline{\bar{u}_i \bar{u}_j} - \bar{u}_i \bar{u}_j$$

$$C_{ij} = \overline{\bar{u}_i u'_j} + \overline{\bar{u}_j u'_i}, and$$

$$R_{ij} = \overline{u'_i u'_j} \tag{9}$$

The Leonard stresses represent interactions between the resolved scales, which result in SGS contribution and can be computed in terms of the LES field, $\bar{u}$. The cross stresses represent interactions between the resolved and unresolved scales, whereas the SGS Reynolds stresses represent interactions between small (unresolved) scales. Only C_{ij} and R_{ij} need to be modeled and the Smagorinsky model is, therefore, applied only to the traceless part of $C_{ij} + R_{ij}$, while L_{ij} is computed explicitly. In this formulation, one does need to know explicitly what the 'filter' function is, since it is needed in the formulation [1, 2]. Smagorinsky model, though very popular, has some notable drawbacks: (a) it requires an input model coefficient, C_s , which is flow dependent, and varies in time and space; (b) it is absolutely dissipative, and can not account for backscatterring (it assumes that energy is only transferred from large to small scales [6]). Dynamic models, which are capable of removing some of the drawbacks of the Smagorinsky

model, are suitable alternatives. In these models, C_s (in the subgrid eddy-viscosity) is not an arbitrary constant specified a priori, but it is calculated during the computational processes [2, 6].

COMPUTATIONAL METHODOLOGIES

In this work, the computational domain is a cubic cavity (of length L_i), with a uniform velocity (U_L) condition at the top. The coordinate system used is Cartesian (x, y, z), where x is aligned with the flow direction, y is vertical, and z is perpendicular to the xy-plane (figure 1). Different cases studied here are described in Table 1. The computational grid used was non-uniform in all three-dimensions, where the grid points were clustered near the walls. Grid resolution study was performed considering four different grid arrangements. Table 2 shows the applied grid arrangements for case two. The mean values of streamwise velocity (U), lateral velocity (W), and lateral vorticity at the centerlines of the cavity are compared (figure 2). Based on these comparisons, the third grid arrangement was selected for the simulation of case two. For code verification purposes, jet penetration and mixing characteristics of multiple jets in a cross flow on a flat plate at three different velocity ratios was investigated.

The results showed better agreement with the experimental measurements of Ajersch et al., in comparison with their own RANS results (see [7]). The following algebraic equation in x-, y-, and z-directions is used for grid stretching near the walls:

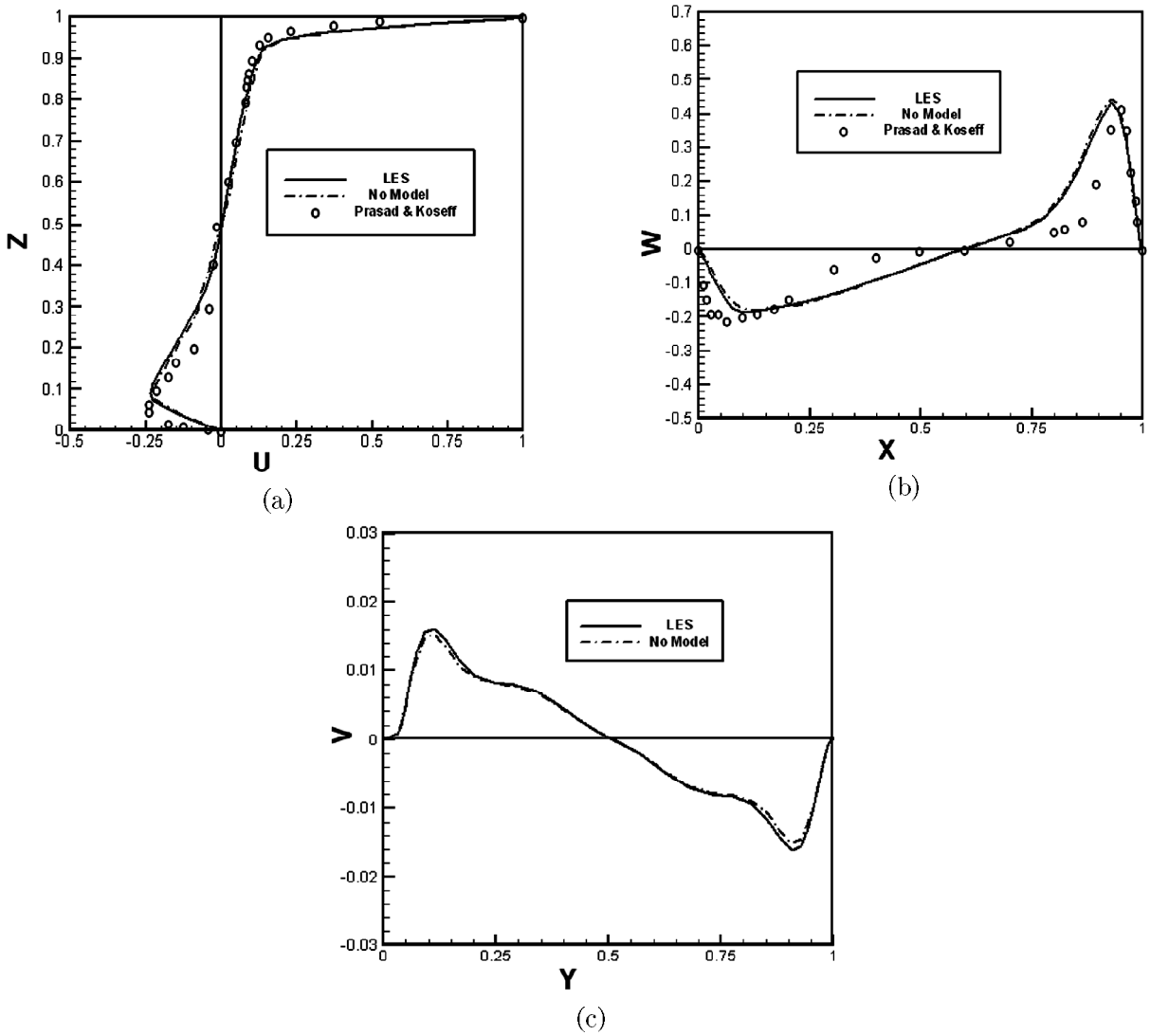

Figure 3. Time-averaged velocity profiles at different centerlines for case 1: (a) streamwise velocity profile at x=0.5; y=0.5 line, (b) vertical velocity profile at y=0.5; z=0.5 line, and (c) lateral velocity profile at x=0.5; z=0 line.

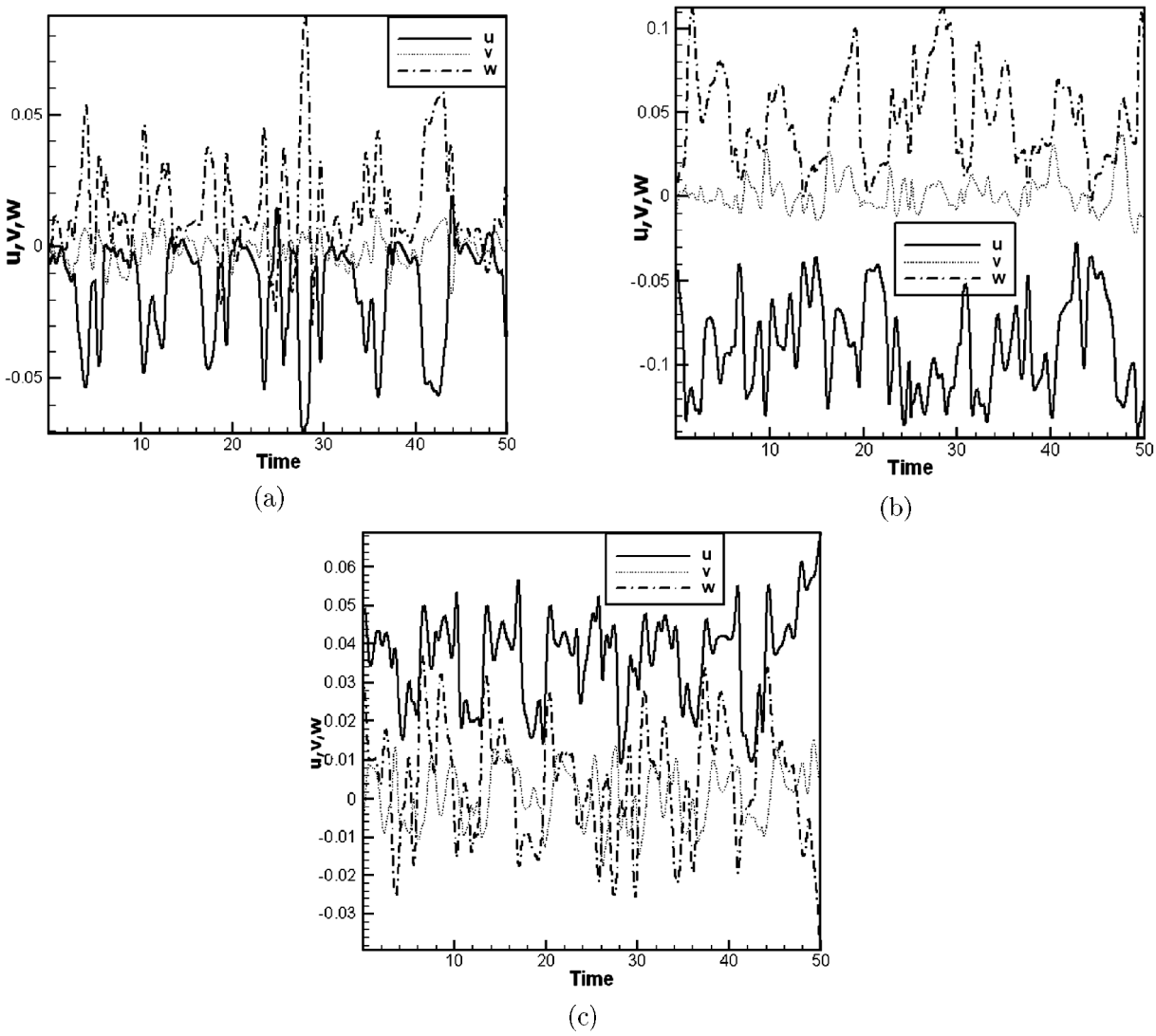

Figure 4. Time evolution of streamwise, lateral and spanwise velocity profiles at three different points for case 2: (a) cavity center point (x=0.5, y=0.25, and z=0.5), (b) laterally spaced from the cavity center point (x=0.5, y=0.25, and z=0.256), and (c) laterally spaced from the cavity center point (x=0.5, y=0.25, and z=0.745).

$$x_i = L_i \frac{(2\alpha+\beta)\left[(\beta+1)/(\beta-1)\right]^{(\eta-\alpha)/(1-\alpha)} + 2\alpha - \beta}{(2\alpha+1)\left\{1+\left[(\beta+1)/(\beta-1)\right]^{(\eta-\alpha)/(1-\alpha)}\right\}} \tag{10}$$

in which, η and β are the metric and the clustering coefficient, respectively. Also, α introduces the clustering position. The minimum and maximum grid spacing are given in Table 2 for case 2.

An incompressible finite volume method, using unsteady SIMPLE algorithm, and implying a staggered grid arrangement was used in this study. It should be noted that the subgrid scale term in the momentum equation was considered as the source term in the unsteady SIMPLE algorithm. Therefore, there are no changes in this algorithm except in the source term. All spatial terms in the Navier-Stokes equations were discretized using Power-Law scheme. Time averaging was used with a constant time step of 0.01 second for 4500 time steps. To discretize the grid scale filter, we employed the box filter in physical space with the trapezoidal rule and linear interpolation. The length scale of the grid filter was equal to the grid size.

RESULTS

LES of an incompressible flow in a three-dimensional cavity at different Reynolds numbers, including 3,200 and 10,000, were performed using the Smagorinsky SGS model. The Reynolds number was based on the lid driven velocity, U_B , and the cavity length, B. Previous experiments have shown that, at Reynolds numbers

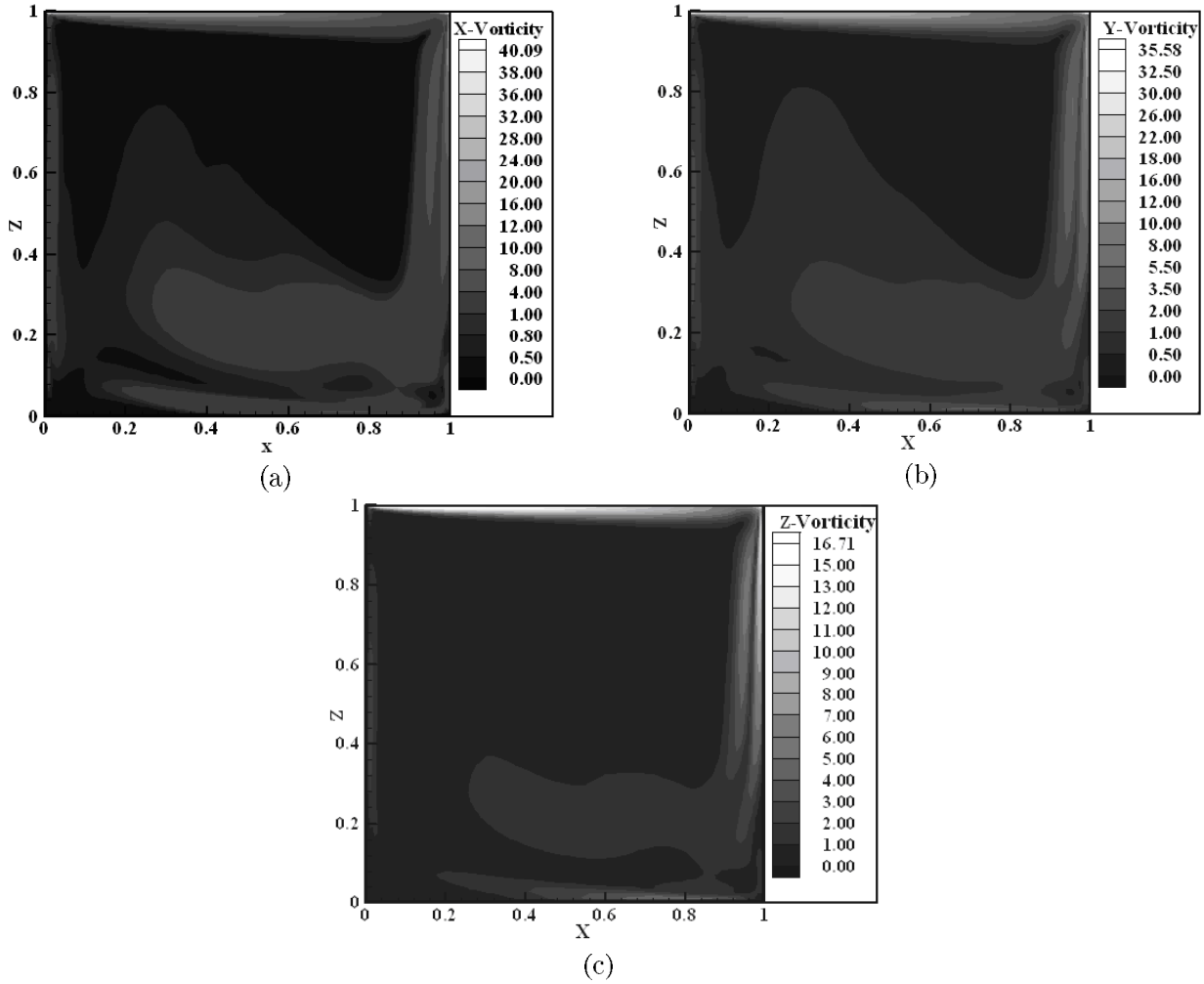

Figure 5. Contours of the ratio of turbulent viscosity to the kinematic viscosity at y=0.25 plane for case 2: (a) x-component, (b) y-component, and (c) z-component.

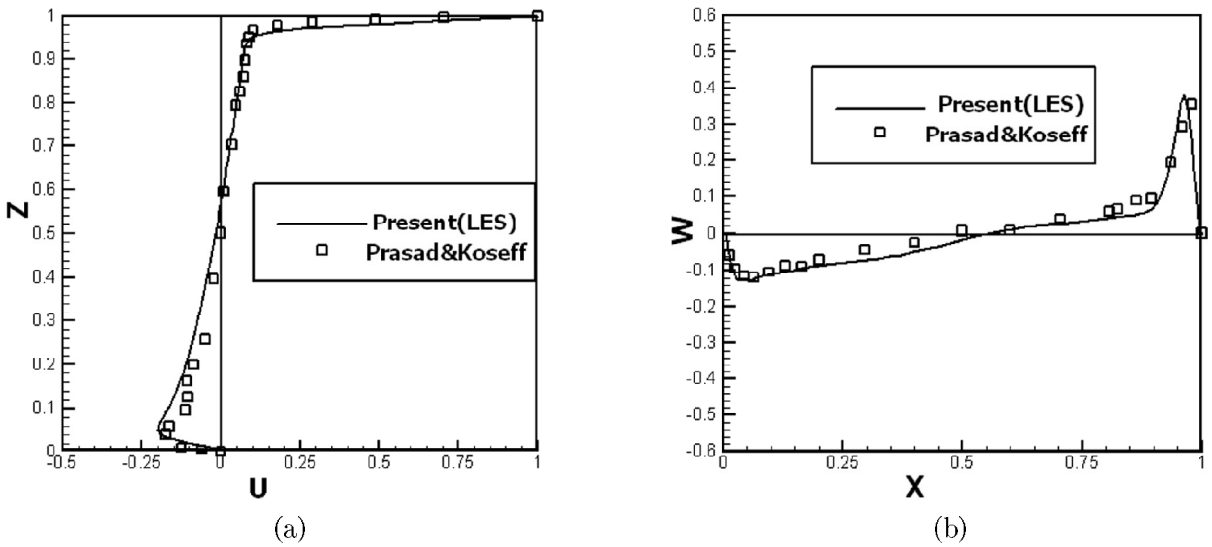

Figure 6. Time-averaged velocity profiles at different centerlines for case 2: (a) streamwise velocity profile at x=0.5; y=0.5 line and (b) vertical velocity profile at y=0.5; z=0.5 line.

lower than 5,000, flow is essnetially laminar although inherent unsteadinesses may occur. At Reynolds numbers higher than about 6,000, flow becomes unstable near the downstream eddy. As the Reynolds number further increases, the flow becomes increasingly turbulent near the walls, and at Reynolds numbers higher than 10,000, the flow near the downstream eddy becomes fully turbulent [8]. Therefore, the two cases considered in the present work are in the laminar and locally turbulent regimes, respectively.

Figures 3(a), 3(b), and 3(c) show the computed mean dimensionless velocities $<\bar{U}>/U_B$, $<\bar{W}>/U_B$ and $<\bar{V}>/U_B$ at the centerlines in horizontal, vertical and spanwise directions for case 1 and are compared with measurements of Prasad and Koseff [8]. Also, the results obtained without using any SGS model are shown in those figures. Both computed profiles agree extremely well with each other and are in good agreements with experimental data. This shows that, the effect of the SGS model diminishes when the flow is essentially laminar [8, 9, 10]. In figures 3(a) and 3(b), we note that, the magnitude of the peak of the velocities was predicted correctly, but the thickness and the maximum velocities at the boundary layers were slightly over-predicted. In figure 3(c), the two computed profiles of velocity in y-direction were shown and again they are in good agreements.

In figures 4(a), (b), and (c), the time evolution of streamwise, lateral and spanwise velocity profiles at three different points, namely, cavity center point (x=0.5, y=0.25, and z=0.5) and two laterally spaced from the cavity center point (z=0.256 and z=0.745) are shown. These profiles are highly non-linear.

In figures 5(a), (b), and (c), the contours of ratio of turbulent viscosity to kinematic viscosity at y=0.25 plane are shown. As it can be seen form these figures, the maximum turbulent viscosity occurs at the top lid (z=0.0) and at x=1.0 wall. The maximum viscosity ratio in x-, y-, and z-directions are 40.09, 35.58, and 16.71, respectively, close to z=1.0 plane near x=0.0 and x=1.0 walls.

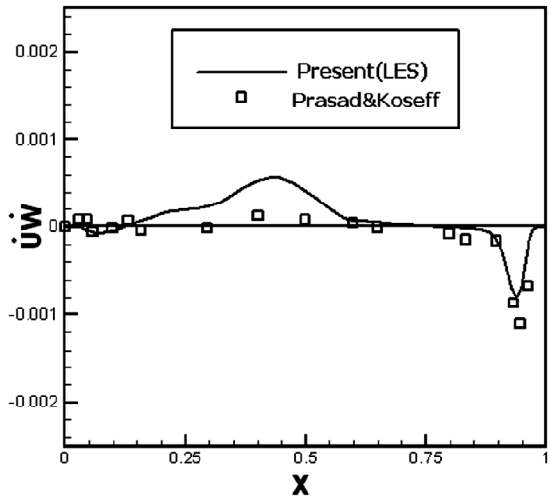

Figure 8. The Reynolds stress 500* $<U'W'>/U_B{}^2$ profile on y=0.5, z=0.5 line for case 2.

Figures 6(a), (b), and (c) show the computed mean dimensionless velocities $<\bar{U}>/U_B$ and $<\bar{W}>/U_B$ at the centerlines in horizontal and vertical directions for case 2 and are compared with measurements of Prasad and Koseff [8]. At this Reynolds number, the flow has become turbulent near the downstream eddy.

The computed centerline mean streamwise and lateral velocity profiles agree well with experiment. It should be noted that the magnitude of the peak of the velocities was predicted correctly, but the thickness and the maximum velocities at the boundary layers were

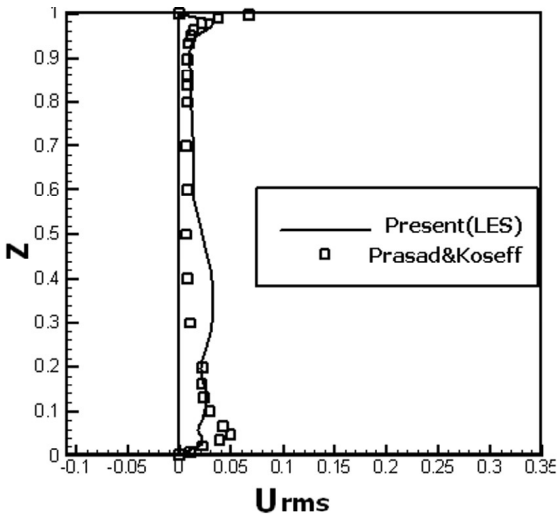

(a)

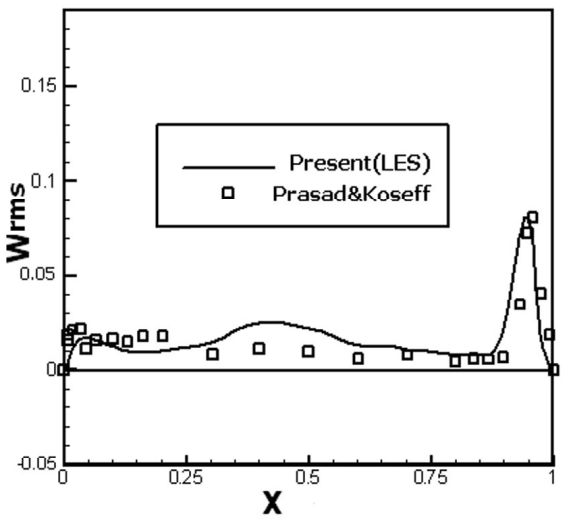

(b)

Figure 7. Root-mean-square (rms) velocities for case 2: (a) U_{rms} at x=0.5; y=0.5 line and (b) W_{rms} at y=0.5; x=0.5 line.

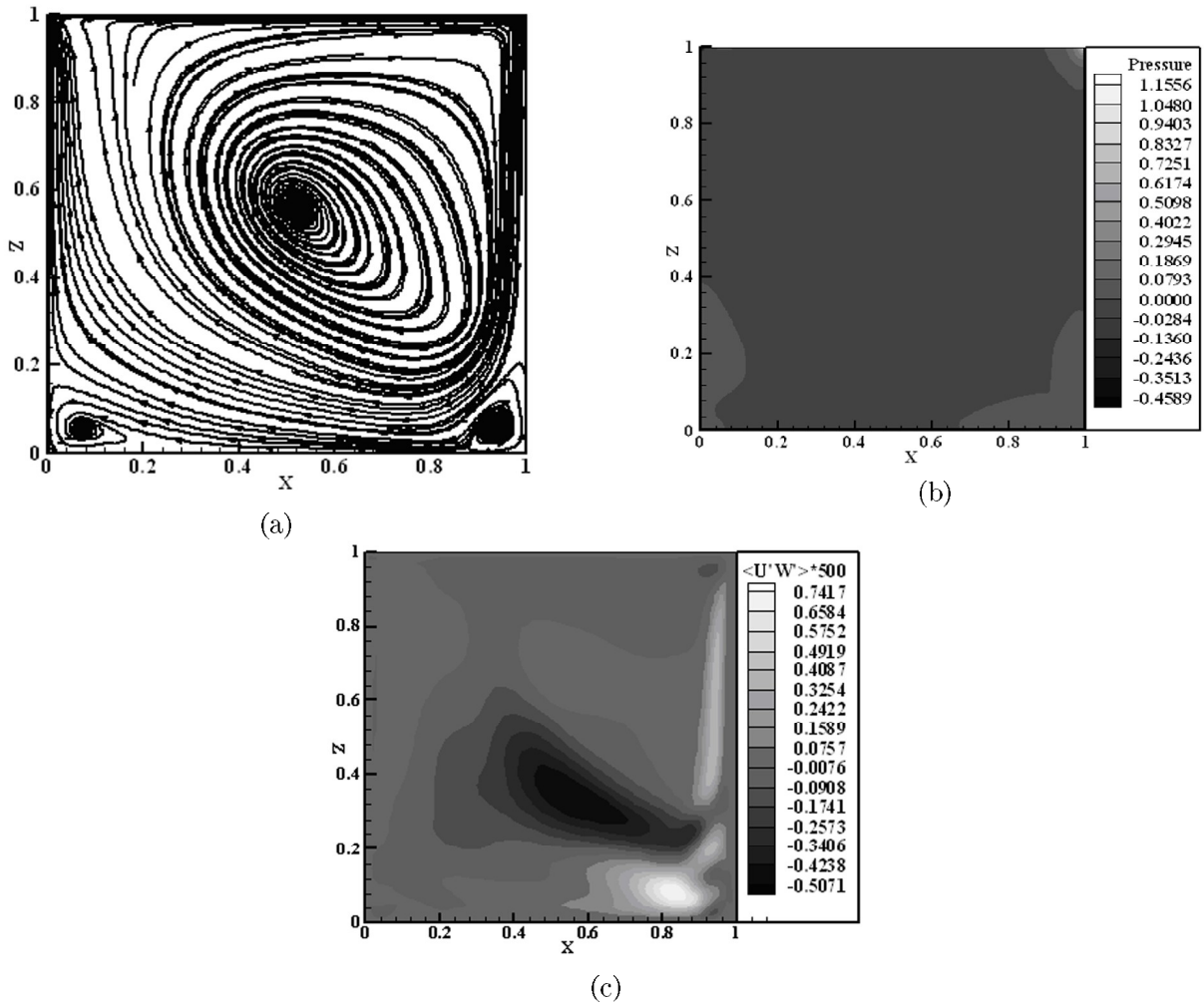

Figure 9. Time-averaged isolines of velocity, pressure, and Reynolds stress at Y=0.25 plane for case 2: (a) <U>-<W > streamlines, (b) pressure, and (c) Reynolds stress (500* $\langle U'W' \rangle$).

negligibility over-predicted. In figures 7(a) and (b), the root-mean-square (rms) velocities $\sqrt{\langle U'^2 \rangle}/U_B$ and $\sqrt{\langle W'^2 \rangle}/U_B$ at the horizontal and vertical centerlines are shown and compared with experimental data. Note, $U_i' = U_i - \langle U_i \rangle$. In figure 7(a), the peak of U_{rms} profile was under-predicted near the bottom wall and the top lid. In figure 7(b), again, the peak of the W_{rms} was under-predicted near the downstream wall although it was shifted to the right.

In figure 8, the Reynolds stress (500* $\langle U'W' \rangle/{U_B}^2$) profile at y=0.5, z=0.5 line for case 2 is shown. Note, the Reynolds stress being discussed is the conventional time averaged one and should be distinguished from the SGS Reynolds stress (τ_{ij}) , defined in equation (4). The computed Reynolds stress was under-predicted near the top lid and was shifted to the left. Also, it was over-predicted near at the cavity center. As, it was stated before, one of the drawbacks of Smagorinsky model is that it is more dissipative near the boundaries and, therefore, the under-prediction of the Reynolds stresses near the top lid is reasonable. This under-prediction may be corrected using a suitable dynamic SGS model.

In Figure 9, the time-averaged isolines of velocity, pressure, and Reynolds stress are shown at Y=0.25 plane. In figure 9(a), the time-averaged isolines of velocity (streamlines of streamwise and normal velocities) are shown. In this plane, three vortices are observed: one near the center and the others at the bottom corners. In figure 9(b), the isolines of pressure are shown. From this figure, it is clear that, the points of minimum and maximum pressure are at the top left and right corners, respectively. Note also that, the pressure distribution is obtained from the SIMPLE algorithm. In figure 9(c), the isolines of Reynolds stress (500* $\langle U'W' \rangle$) are shown. It is observed that the region between the vortices has the maximum and minimum Reynolds stresses. It should be noted that the grid refinement required for satisfying the

Kolmogorov length scale is proportional to $Re^{\frac{3}{4}}$ nodes in each direction (for DNS approach). For most grid arrangements, this grid requirement is inaccessible, because of CPU time and memory capacity. Even though the present grid cannot resolve the Kolmogorov scale very well, it can resolve the scales significantly in the flow as seen from the mean-velocity, rms-velocity and Reynolds stresses obtained from the LES approach. Therefore, the small differences between the computed results and the experimental data are probably due to bad behavior of the Smagorinsky model near the walls [9].

CONCLUSION

LES of an incompressible flow in a three-dimensional cavity was performed using Smagorinsky model. Two cases at different Reynolds numbers, including 3,200 and 10,000 were studied and the computed mean velocities, root-mean-square (rms) velocities, and the Reynolds stresses were shown on the centerlines of the cavity and were compared with the experimental data of Prasad and Koseff. These comparisons showed reasonably acceptable agreements within the approximations. However, the mean and the rms velocities were slightly under-predicted near the walls and near the top lid. Also, the thickness and the maximum velocities of the boundary layers were slightly over-predicted and the Reynolds stress profiles were under-predicted near the top lid. Moreover, maximum turbulent viscosity in x-, y-, and z-directions occurs close to z=1.0 plane near the x=0.0 and x=1.0 walls.

REFERENCES

1. Piomelli U., "Large-Eddy Simulation of Turbulent Flows", *Short Course*, Department of Mechanical Engineering, University of Maryland, USA, (1994).
2. Ghosal, S., , "Mathematical and Physical Constrains on LES", *AIAA Paper*, PP 98-2803(1998).
3. Ghosal S. and Moin P., "The Basic Equation for Large Eddy Simulation of Turbulent Flow in Complex Geometry", *J. Comp. Phy.*, **118**, PP 24-37(1995).
4. Tafti, D.K., Zhang, X., Huang, W., and Wang, G., "Large-Eddy Simulations of Flow and Heat Transfer in Complex Three-Dimensional Multilouvered Fins", *ASME Fluids Engineering Division Summer Meeting*, Boston, Massachusetts, USA, FEDSM2000-11325, (2000).
5. Peyret R., *Handbook of Computational Fluid Mechanics*, Academic Press Limited, (1996).
6. Sohankar A. and Davidson L., "Large Eddy Simulation of Turbulent Flow over a Square Prism by Using two Subgrid-Scale Models", 4th International and 8th Annual Conference of Iranian Society of Mechanical Engineers, (2000).
7. Ramezani-Zadeh M. and Taeibi-Rahni M., "Large Eddy Simulation of Multiple Jets in a Cross flow Using Smagorinsky Model", *ISME 2001*, Guilan University, Rasht-Iran, PP 293-299(2001).
8. Zang Y., Street R.L., and Koseff J.R, "A Dynamic Mixed Subgrid-Scale Model and its Application to Turbulent Recirculating Flows", *Phys. Fluids A*, **5**(12), (1993).
9. Jimenez, J. and Moser, R., "LES: Where Are We and What We Can Expect?", *AIAA Paper*, PP 98-2850(1998).
10. Deshpande, M.D. and George Milton, S., "Kolmogorov Scales in a Driven Cavity Flow", *Fluid Dynamics Research*, **22**, PP 359-381(1998).